Communication

The Electronic Origin of the Visible-Light Absorption Properties of C-, N- and S-Doped TiO Nanomaterials

Xiaobo Chen, and Clemens Burda

J. Am. Chem. Soc., **2008**, 130 (15), 5018-5019 • DOI: 10.1021/ja711023z • Publication Date (Web): 25 March 2008

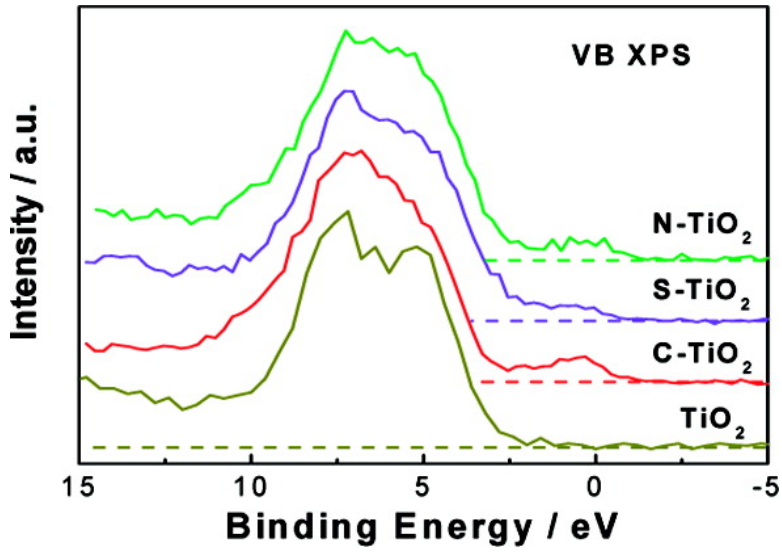

More About This Article

Additional resources and features associated with this article are available within the HTML version:

- Supporting Information
- Links to the 4 articles that cite this article, as of the time of this article download
- Access to high resolution figures
- Links to articles and content related to this article
- Copyright permission to reproduce figures and/or text from this article

View the Full Text HTML

J|A|C|S
COMMUNICATIONS

Published on Web 03/25/2008

The Electronic Origin of the Visible-Light Absorption Properties of C-, N- and S-Doped TiO_2 Nanomaterials

Xiaobo Chen† and Clemens Burda*

Center for Chemical Dynamics & Nanomaterials Research Department of Chemistry, Case Western Reserve University, Cleveland, Ohio 44106

Received December 11, 2007; E-mail: cxb77@case.edu

Titanium dioxide (TiO_2) has been widely used as a pigment since as early as 1916[1] and considered as the most promising photocatalyst in environmental cleanup, mainly stimulated by the discovery of its water splitting activity under ultraviolet (UV) light in the early 1970s.[2] However, its limited UV-driven activity largely inhibits its overall efficiency under natural sunlight, which consists of 5% UV (300–400 nm), 43% visible (400–700 nm), and 52% infrared (700–2500 nm).[3] One of the potential solutions for improving its efficiency is to shift its absorption from the UV region into the visible-light region, allowing for more photons to be absorbed and utilized in decomposing the pollutants. Much progress has been made in the area of visible-light-active TiO_2 by introducing various dopants into its lattice, including metal[4] and nonmetal elements.[5]

The optical properties of a material are primarily the reflections of its intrinsic electronic structure such as the transitions from an occupied electronic level to another empty level. As for pure and perfect semiconductors, they are transitions from the valence band to the conduction band. When dopants and defects are introduced, additional extrinsic electronic levels can be located in the energy band gap of the metal oxide. The valence band edge of TiO_2 primarily derives from oxygen 2p orbitals and the conduction band edge from titanium 3d orbitals. For nonmetal light-element dopants, the modified optical properties are in general due to the electronic transitions from the dopant 2p or 3p orbitals to Ti 3d orbitals. However, the discussion on the exact nature and energetic positioning of these dopant levels and how much modification these dopants bring in has not reached a settlement from both the theoretical and experimental point of view. For example, the nitrogen dopant was found to add shallow mixed states near the valence band in some studies,[5a,6] while in other studies, different conclusions were made, partially due to the reflection of the different aspects of doped TiO_2 and the shortcoming of each theoretical and experimental method.[7] The discrepancy actually provided complementary information on the complicated nature of the properties of doped nanomaterials. In this study, we present the experimental observation of the electronic structures of main-group element doped TiO_2 nanomaterials using X-ray photoelectron spectroscopy (XPS). In addition, valence band XPS was used for the observation of extra electronic states above the valence band of TiO_2. These results suggest that main-group element doping of TiO_2 leads in general to an increase of the density of states just above the TiO_2 valence band edge and to visible-light absorption.

The doped TiO_2 nanomaterials were prepared with a high-temperature oxidation method by oxidizing titanium carbide, nitride, and sulfide powders at 350− 650 °C in air for a certain time. The samples were crystalline. Figure 1A shows the X-ray diffraction (XRD) patterns of the pure (Degussa P25) and doped TiO_2 obtained. P25 is composed of 75–80% anatase phase and 20–25% rutile phase, with average size of 25 nm, and is used here as a reference. The C- and S-doped TiO_2 nanomaterials displayed an anatase phase with an average size of 25 nm in diameter, and the N-doped TiO_2 had a rutile phase with size of 70 nm, calculated with the Scherrer equation. Figure 1B shows the transmission electron microscopy (TEM) images of the C-doped TiO_2 nanomaterial. Its average size was around 25 nm. The selected area electron diffraction pattern and high-resolution TEM confirmed its highly crystalline anatase structure. The overall surface C, S, and N dopant concentrations were found to be 0.5, 4.2, and 0.2% in atomic percent from the atomic XPS (see Supporting Information). The dopant level in these samples could be adjusted via the sintering time.

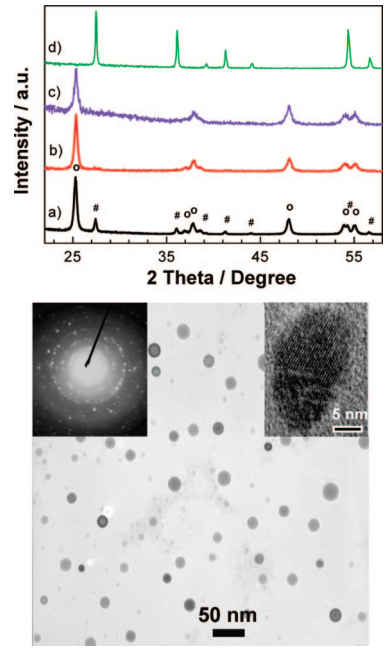

Figure 1. (A) XRD patterns of (a) pure TiO_2 (anatase phase labeled with o, rutile with #), (b) C-TiO_2, (c) S-TiO_2, (d) N-TiO_2. (B) TEM image of C-TiO_2. The insets show the selected area electron diffraction pattern (left) and high-resolution TEM (right).

All these doped TiO_2 nanomaterials show a yellow to light yellow color, suggesting their ability to absorb light in the visible region. Figure 2 shows the diffuse reflectance spectra of these materials. P25 shows a band-edge absorption around 390 nm (3.2 eV), which is typical for anatase phase. Both C- and

† Current address: Lawrence Berkeley National Laboratory, University of California at Berkeley, CA 94720.

10.1021/ja711023z CCC: $40.75

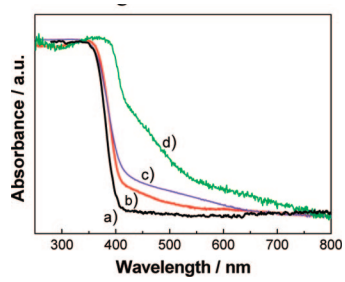

Figure 2. Diffuse reflectance spectra of (a) pure TiO_2, (b) C-TiO_2, (c) S-TiO_2, (d) N-TiO_2.

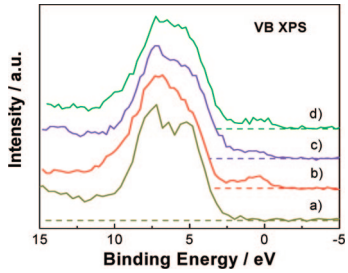

Figure 3. VB XPS spectra of (a) pure TiO_2, (b) C-TiO_2, (c) S-TiO_2, and (d) N-TiO_2.

S-doped TiO_2 nanomateirals showed band-edge absorptions around 390 nm (3.2 eV), and N-doped TiO_2 nanomaterial showed a 3.0 eV (415 nm) rutile-phase band-edge absorption. The band-edge absorption difference can be attributed to the crystal phase differences. Compared to pure TiO_2, additional absorptions up to 800 nm were observed for the C-, S-, and N-doped nanomaterials. The improved absorption can be divided into roughly two parts: 415−550 nm (shoulder) and 550 ∼ 800 nm (tail) for N-doped TiO_2, 390–490 nm (shoulder) and 490 ∼ 800 nm (tail) for C-doped TiO_2, and 390 ∼ 800 nm (tail) for S-doped TiO_2. Among the three, the modification of the optical properties is the largest for N-doped TiO_2, although its dopant concentration is the lowest.

In XPS, not only the information on the binding energy of a specific element can be obtained but also the total density of states (DOS) of the valence band (VB).[8] Figure 3 shows the valence band XPS spectra of the C-, S-, and N-doped TiO_2 nanomaterials. Additional diffusive electronic states were observed above the valence band edge of pure TiO_2. These additional states induced by the C, N, and S dopants were derived by fitting the data with Gaussian functions (see Supporting Information) in comparison with Degussa P25 and previous theoretical calculations.[5a] These states can be attributed to the C 2p, S 3p, and N 2p orbitals in the doped TiO_2. In general, they add deeper states into the band gap in the order of C > N > S. This finding is consistent with the conclusion from previous theoretical and experimental studies.[5a,6a,9] Band-center states were observed for C- and N-doped TiO_2, for S-TiO_2, only very diffusive states were observed. Their diffused features reflected both the electronic effect and structural-induced effect from the dopants and the diffused dopant's sites in the TiO_2 lattice. For example, from the atomic N 1s XPS spectra, both substitutional (around 397.0 eV) and interstitial sites (400.0 eV) were observed, which would induce multicenter states (if the spectra were well-resolved) or diffused states (if not well-resolved). The additional more diffused states brought by the S dopant can be attributed to the weaker structural and electronic modification of TiO_2 compared to the C and N dopant, where more electronic effects were seen due to the additional breakdown of charge balance of the TiO_2 lattice. The optical transitions between these dopants and dopant-induced levels and Ti 3d orbitals explain the observed visible-light absorptions of these main-group element doped TiO_2 nanomaterials. The observed "shoulder" and "tail-like" features in the UV–vis spectra are directly related to the above modification of the electronic states from the dopants. However, their exact match is not straightforward, due to the different transition probabilities in the UV–vis and XPS spectra.

In summary, our research effort on the electronic origins of the visible-light absorption properties of a series of nonmetal doped TiO_2 nanomaterials has revealed additional electronic states above the valence band edge of pure TiO_2 for C-, N-, and S-doped TiO_2 nanomaterials via XPS. This additional electron density of states can explain the red-shifted absorption of these potential photocatalysts and simultaneously their lowered oxidation potentials.

Acknowledgment. The authors greatly appreciate the support from ACS-PRF (# 45359-AC10) and NSF (#CHE-0239688).

Supporting Information Available: Atomic XPS for pure, C-, S-, and N-doped TiO_2 and fits of the VB XPS spectra. This material is available free of charge via the Internet at http://pubs.acs.org.

References

(1) (a) Pfaff, G.; Reynders, P. *Chem. Rev.* **1999**, *99*, 1963–1981. (b) Hoffmann, M. R.; Martin, S. T.; Choi, W.; Bahnemann, D. W. *Chem. Rev.* **1995**, *95*, 69–96. (c) Linsebigler, A. L.; Lu, G.; Yates, J. T., Jr *Chem. Rev.* **1995**, *95*, 735–758. (d) Millis, A.; Le Hunte, S. *J. Photochem. Photobiol. A* **1997**, *108*, 1–35. (e) Chen, X.; Mao, S. S. *Chem. Rev.* **2007**, *107*, 2891–2959. (f) Bavykin, D. V.; Friedrich, J. M.; Walsh, F. C. *Adv. Mater.* **2006**, *18*, 2807–2824. (g) Cozzoli, P. D.; Pellegrino, T.; Manna, L. *Chem. Soc. Rev.* **2006**, *35*, 1195–1208.

(2) (a) Fujishima, A.; Honda, K. *Nature* **1972**, *238*, 37–38. (b) Fujishima, A.; Rao, T. N.; Tryk, D. A. *J. Photochem. Photobiol. C* **2000**, *1*, 1–21. (c) Tryk, D. A.; Fujishima, A.; Honda, K. *Electrochim. Acta* **2000**, *45*, 2363–2376.

(3) Levinson, R.; Berdahl, P.; Akbari, H. *Sol. Energy Mater. Sol. Cells* **2005**, *89*, 319–349.

(4) (a) Choi, W.; Termin, A.; Hoffmann, M. R. *Angew. Chem.* **1994**, *106*, 1148–1149. (b) Umebayashi, T.; Yamaki, T.; Itoh, H.; Asai, K *J. Phys. Chem. Solids* **2002**, *63*, 1909–1920. (c) Anpo, M.; Kishiguchi, S.; Ichihashi, Y.; Takeuchi, M.; Yamashita, H.; Ikeue, K.; Morin, B.; Davidson, A.; Che, M. *Res. Chem. Intermed.* **2001**, *27*, 459–467.

(5) (a) Asahi, R.; Morikawa, T.; Ohwaki, T.; Aoki, K.; Taga, Y. *Science* **2001**, *293*, 269–271. (b) Khan, S. U. M.; Al-Shahry, M.; Ingler, W. B., Jr *Science* **2002**, *297*, 2243–2245. (c) Burda, C.; Lou, Y.; Chen, X.; Samia, A. C. S.; Stout, J.; Gole, J. L. *Nano Lett.* **2003**, *3*, 1049. (d) Chen, X.; Burda, C. *J. Phys. Chem. B* **2004**, *108*, 15446–15449. (e) Chen, X.; Lou, Y.; Samia, A. C. S.; Burda, C.; Gole, J. L. *Adv. Funct. Mater.* **2005**, *15*, 41–49.

(6) (a) Nakamura, R.; Tanaka, T.; Nakato, Y. *J. Phys. Chem. B* **2004**, *108*, 10617–10620. (b) Wang, Y.; Doren, D. J. *Solid State Commun.* **2005**, *136*, 186–189.

(7) (a) Lee, J. Y.; Park, J.; Cho, J. H. *Appl. Phys. Lett.* **2005**, *87*, 011904/1–011904/3. (b) Nakano, Y.; Morikawa, T.; Ohwaki, T.; Taga, Y. *Appl. Phys. Lett.* **2005**, *86*, 132104/1–132104/3. (c) Okato, T.; Sakano, T.; Obara, M. *Phys. Rev. B* **2005**, *72*, 115124/1–115124/6.

(8) (a) Hüfner, S. *Photoelectron Spectroscopy: Principles and Applications*; Springer-Verlag: New York, 1995. (b) Cardona, M.; Ley, L. *Photoemission in Solids I General Principles*; Springer-Verlag: New York, 1978. (c) Ley, L.; Cardona, M. *Photoemission in Solids II: Case Studies*; Springer-Verlag: New York, 1979. (d) Woicik, J. C.; Nelson, E. J.; Kronik, L.; Jain, M.; Chelikowsky, J. R.; Heskett, D.; Berman, L. E.; Herman, G. S *Phys. Rev. Lett.* **2002**, *89*, 077401/1–077401/4.

(9) (a) Lindgren, T.; Lu, J.; Hoel, A.; Granqvist, C. G.; Torres, G. R.; Lindquist, S. E. *Solar Energy Mater. Solar Cells* **2004**, *84*, 145–157. (b) Umebayashi, T.; Yamaki, T.; Itoh, H.; Asai, K. *Appl. Phys. Lett.* **2002**, *81*, 454–456.

JA711023Z